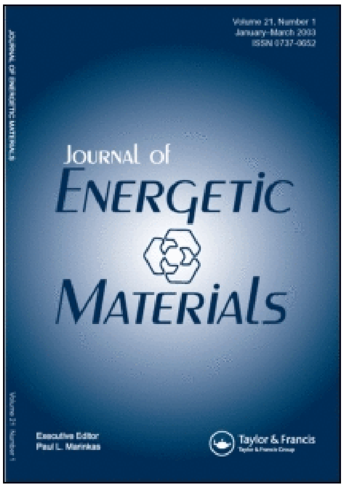

Journal of Energetic Materials
Publication details, including instructions for authors and subscription information:
http://www.informaworld.com/smpp/title~content=t713770432

Particle Size Effects on Thermal Decomposition of Energetic Material

M. Fathollahi[a]; S. M. Pourmortazavi[a]; S. G. Hosseini[a]

[a] Faculty of Material and Manufacturing Technologies, Malek Ashtar University of Technology, Tehran, Iran

To cite this Article Fathollahi, M. , Pourmortazavi, S. M. and Hosseini, S. G.(2008) 'Particle Size Effects on Thermal Decomposition of Energetic Material', Journal of Energetic Materials, 26: 1, 52 — 69

To link to this Article: DOI: 10.1080/07370650701719295

URL: http://dx.doi.org/10.1080/07370650701719295

Journal of Energetic Materials, 26: 52–69, 2008

ISSN: 0737-0652 print/1545-8822 online
DOI: 10.1080/07370650701719295

Particle Size Effects on Thermal Decomposition of Energetic Material

M. FATHOLLAHI
S. M. POURMORTAZAVI
S. G. HOSSEINI

Faculty of Material and Manufacturing Technologies,
Malek Ashtar University of Technology, Tehran, Iran

This work refers to a study of the thermal decomposition of octahydro-1,3,5,7-tetranitro-1,3,5,7-tetrazocine (HMX) by differential scanning calorimetry (DSC) under non-isothermal conditions, with heating rates from 5 to $20^{\circ}C\,min^{-1}$*. The influence of the particle size in the thermal decomposition of HMX was verified. The activation energy for the decomposition of each sample was calculated using the peak temperature shift methods, proposed by Kissinger and Ozawa. A significant variation in the results was observed according to the range of the particle size used. The results showed that, as the particle size of HMX increased, the thermal decomposition temperature of HMX and the decompositional activation energies ranges enhanced. At the same time, at a constant heating rate, the decomposition temperatures of the smaller particles were lower than those of larger ones. The critical temperature for thermal explosion of each sample was calculated. Also, the values of* $\Delta S^{\#}$*,* $\Delta H^{\#}$*, and* $\Delta G^{\#}$ *of reaction for each particle size were computed.*

Keywords: activation energy, DSC, energetic material, HMX, kinetic parameters, Kissinger, Ozawa, particle size effect, thermal decomposition

Address correspondence to S. M. Pourmortazavi, P.O. Box 16765–3454, Tehran, Iran. E-mail: pourmortazavi@yahoo.com

Introduction

HMX (octahydro-1,3,5,7-tetranitro-1,3,5,7-tetrazocine) is a high explosive used in many plastic-bonded explosives (PBX), double base propellants, and propellant composites because of its high calorific potential, high density, and smokeless combustion products [1,2]. The thermal decomposition of HMX has been the subject of extensive studies for many years and its complexity, dependence on the experimental conditions, physical state, temperature, pressure, etc., are well known [3,4]. A knowledge of its decomposition kinetics enables the previous information required to evaluate critical conditions leading to thermal explosion [5] as well as studies of compatibility with additives [6].

Techniques of thermal analysis such as DTA, TG, and DSC have been largely used in the study of explosive decomposition kinetics in isothermal and nonisothermal conditions [5–8]. Due to the variety of techniques and methods used to calculate these parameters for HMX, there is a wide range of activation energy values found in literature varying from 229 to 429 kJ mol^{-1} [9].

The aim of this work was to derive the kinetic parameters of the decomposition computed using nonisothermal differential scanning calorimetry and applying them to equations based on the variable heating rate methods, as described by Kissinger [10] and Ozawa [11]. The effect of particle size on its thermal decomposition was also studied.

Experimental

This work was performed with a DuPont DSC model 910 at the heating rates of 5, 10, 15, and 20°C min^{-1} from 50°C up to the end of the decomposition. DSC measurements were conducted by placing 0.5–2.5 mg of pure HMX in an aluminum pan with a perforated cover under nitrogen atmosphere (40 mL min^{-1}). Two runs with each sample were made for each heating rate.

The investigations of the decomposition kinetics were done with six standard classes of HMX [12]. The various HMX particle sizes were prepared by recrystallizing saturated solutions

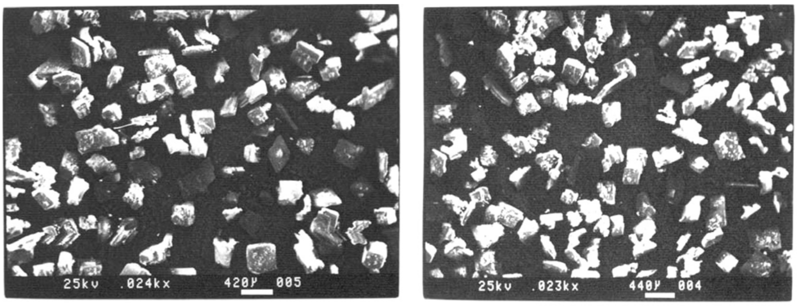

350 µm

40 µm

Figure 1. Scanning electron micrographs of crystals selected from samples 1 and 6 that were subsequently subjected to partial decomposition in the DSC.

(in pure analysis ethanol) of HMX at several thermal programs of cooling. The samples were separated into six fractions (average particle size of 40, 50, 90, 125, 160, and 350 µm) by sieving. The particle size ranges of HMX samples were separated by the screening machine. Particle sizes and purity of the HMX were checked with a Topocon Electron Microscope model SR-50 and a HPLC Instrument. Figure 1 shows photomicrographs for two samples of HMX particles.

Results and Discussion

HMX exists in four solid-phase polymorphs, labeled α -, β-, γ-, and δ-HMX [13,14], each of which can reportedly be prepared by a specific cooling rate of a reaction solution [15]. The β phase of HMX has the highest density and is stable at room temperature; it is the form in which HMX is normally produced and used. However, when heated to temperatures above 162°C, the β phase converts to the δ phase HMX [13,16–19]. This conversion of the β phase (monoclinic lattice structure) to the δ phase (hexagonal lattice structure) involves a major disruption of the cohesive forces in the HMX crystal lattice and a ring conformation change from β (chair) to δ (chair-chair) [20,21]. The electrostatic forces created within the HMX lattice produce a potential energy barrier to overcome in the transformation from the $\beta \rightarrow \delta$ phase [17].

Figure 2 shows DSC curves for sample 4 (90 µm) of HMX at 5, 10, 15, and 20°C min^{-1} heating rates. The curves were presented in the range 260–300°C for better visualization. The DSC curve of HMX shows three peaks. At first, there is a weak endothermic peak observe at about 185–200°C that is due to the morphology transformation ($\beta \rightarrow \delta$). The exact transition temperature for each particle size obviously depends on the rate of heating (180°C at 5°C/min and 190°C at 20°C/min heating rate for sample 4). Usually the crystal phase transformations are reversible and therefore it is tempting to say that the irreversibility in HMX is due to the different conformational structure of HMX molecules in the respective crystal structures [22]. After a transformation step, a sharp endothermic peak at

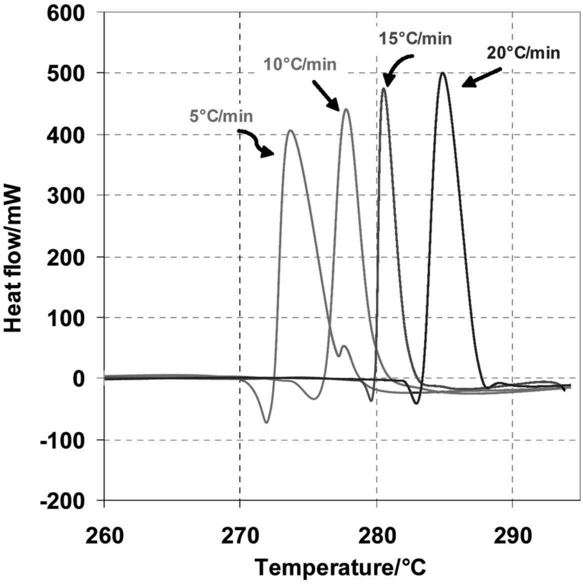

Figure 2. The effect of heating rate on the thermal decomposition of HMX (sample weight 2.0 mg; nitrogen atmosphere and HMX particle size 90 µm).

274–281°Cappears in the DSC curve of HMX that corresponds to the onset of melting. This peak immediately is followed by a strong exothermic peak, which is due to the self-decomposition of HMX [23,24]. HMX decomposition is exothermic.

Figure 3 shows the influence of the heating rate on the peak temperature for sample 4. The behavior of all samples was similar and the onest temperature and maximum heat output temperature rises with increasing heating rate. This phenomenon was observed because decomposition of HMX begins slowly, accelerates in rate during the process, and tapers off until the sample is completely consumed [25,26]. On the other hand, at the constant heating rate, as shown in Fig. 4 the decomposition occurred at lower temperatures by decreasing particle size of HMX samples. Also, Fig. 5 shows this result at heating rate of 20°C/min. This observation may be due to two reasons: (1) The reduced particle size

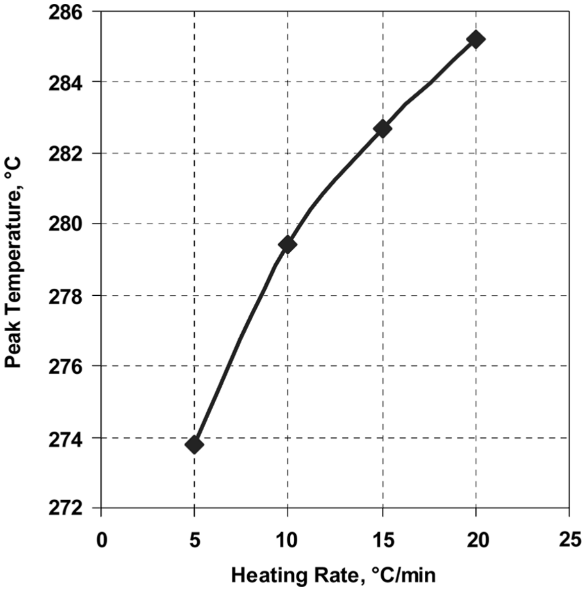

Figure 3. The effect of heating rate of DSC on the peak temperature, T_m, of HMX (90 µm particle size).

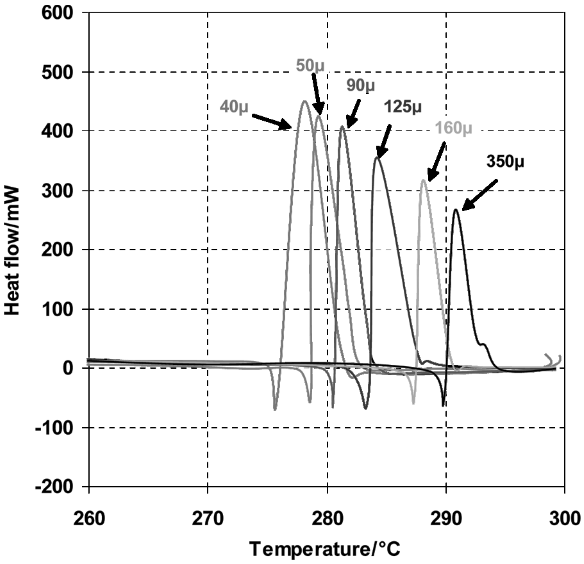

Figure 4. DSC curves of HMX samples with different particle sizes (sample weight 2.0 mg; nitrogen atmosphere and heating rate 20℃/min).

of the HMX sample enhances its surface area, which causes an increase in the sample's heat absorption ability and hence lower decomposition temperature [27]. (2) The formation of localized hotspots is an important step in the ignition of energetic materials [28]. When the particles in an explosive are small and jagged, less thermal energy is needed to produce hot spots. This is because energy is localized at the stress points. Also, dislocations, cracks, and other discontinuities in the crystal structure provide sites favorable to the formation of hot spots. These sites may come about from structural dislocations running between grain boundaries or other discontinuities. These form as a crystal grows and acquires more molecules, which do not fit properly in to the normal pattern. The faults do not heal with continued overgrowth [29,30].

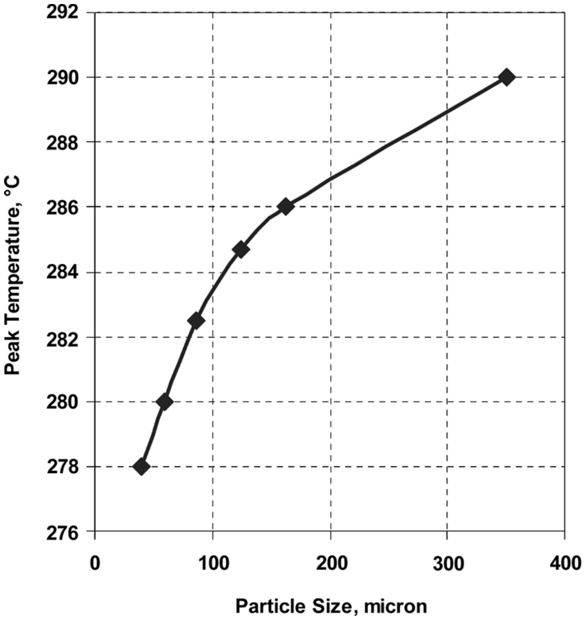

Figure 5. The effect of particle size on the peak temperature, T_m, of the HMX in DSC at a constant heating rate (20°C/min).

Kinetic Parameters

The temperatures of exothermic peak for HMX at different heating rates are shown in Table 1. The kinetic parameters of decomposition for HMX were determined via DSC using Kissinger's method [31–35]. Kissinger's method has been used in the literature to determine the activation energy of solid-state reactions from plots of the logarithm of the heating rate versus the inverse of the temperature at the maximum reaction rate in constant heating rate experiments [10]. The activation energy can be determined by Kissinger's method without a precise knowledge of the reaction mechanism, using the following equation:

$$Ln\frac{(\varphi)}{T^2} = Ln\left(\frac{AR}{T}\right) - \frac{Ea}{RT_P} \tag{1}$$

Table 1

The effect of particle size on the DSC peak temperature and the calculated values of activation energy and pre-exponential factor, as determined by the Kissinger and Ozawa methods for HMX

				Kissinger's method		Ozawa's methods	
Sample no.	Particle size (µm)	Heating rate (°C/min)	T_m (°C)	E (kJ/mol)	Log A (s^{-1})	E (kJ/mol)	Log A (s^{-1})
1	350	5	282.7	419.71	37.62	429.29	38.50
		10	286.2				
		15	290.2				
		20	291.6				
2	160	5	280.3	373.06	33.22	382.34	34.09
		10	284.1				
		15	286.7				
		20	289.5				
3	125	5	277.2	330.72	29.22	339.96	30.09
		10	281.2				
		15	284.5				
		20	287.4				

(*Continued*)

Table 1
Continued

				Kissinger's method		Ozawa's methods	
Sample no.	Particle size (µm)	Heating rate (°C/min)	T_m (°C)	E (kJ/mol)	Log A (s^{-1})	E (kJ/mol)	Log A (s^{-1})
4	90	5	273.8	285.49	24.94	294.69	25.81
		10	279.4				
		15	282.2				
		20	285.8				
5	50	5	271.1	250.17	21.59	259.33	22.49
		10	275.6				
		15	280.1				
		20	284.5				
6	40	5	268.2	229.9	19.67	239.01	20.73
		10	275.1				
		15	278.6				
		20	282.7				

where ϕ is the heating rate and T_P is the peak temperature of a DSC scan at that rate. In the experiments, T_Ps at various rates were collected, and values of ln (φ/T_P^2) were plotted against values of $1/T_P$. A straight line through the data points was obtained by linear regression. The activation energy, E_a, was determined from the slope, and the frequency factor, A, was determined from the intercept. The results are tabulated in Table 1.

Another method that could be used for determination the activation energy without knowledge of reaction order is Ozawa method [36–40]. The activation energy of this reaction was estimated using Ozawa method from a linear fitting of ϕ versus $1/T_p$ in the following equation [32]:

$$\log \beta + 0.456E/RT = C \qquad (2)$$

The activation energy was calculated from the slope. The calculated results of activation energy are shown in Table 1.

A comparison of the activation energies obtained from the Kissinger and Ozawa methods indicates that both methods agree with each other quite well in estimating the reaction activation energies and frequency factors. As shown in Figures 6 and 7, the activation energy and frequency factor calculated from the Kissinger method for each of HMX samples are slightly lower than that calculated from the Ozawa method.

Figures 6 and 7 show the influence of particle size on the results of activation energy and frequency factor calculated by the Ozawa and Kissinger methods. It was observed that the activation energy and frequency factor obtained by the two methods decrease as the particle size of HMX decrease. This is because energy is localized at the stress points and the population of these points increased by formation of smaller particles [30].

Estimation of Critical Temperature for Thermal Explosion

The critical ignition temperature (T_b) is an important parameter required to ensure safe storage and process operations

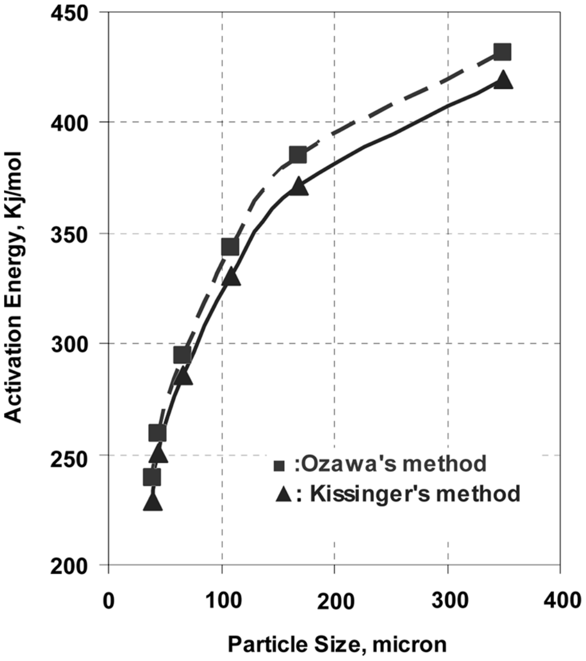

Figure 6. Plot of activation energy vs. particle size for the various HMX samples as calculated by the Kissinger and Ozawa methods.

involving explosives, propellants, and pyrotechnics. It is defined as the lowest temperature to which a specific charge may be heated without undergoing thermal runaway [41,42]. T_b may be calculated from combustion theory and appropriate thermokinetic parameters, namely the activation energy (E), the pre-exponential factor (A), and the heating rate (φ).

The values (T_{p0}) of the peak temperatures (T_p) for each sample corresponding to $\varphi \rightarrow 0$ obtained by Eq. (3) taken from Yang et al. [43] are shown in Table 2.

$$T_{pi} = T_{P0} + b\varphi_i + c\varphi_i^2 + d\varphi_i^3, i = 1, \ldots, 5 \tag{3}$$

where b, c, and d are coefficients.

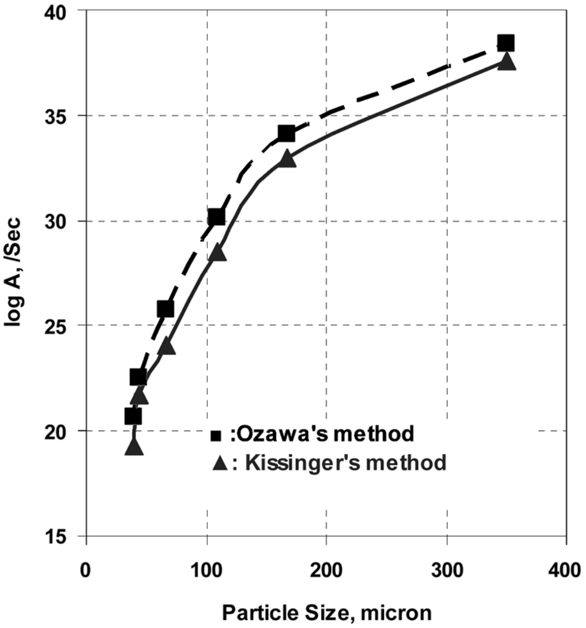

Figure 7. Changes of log *A* values vs. particle size of HMX samples obtained by the Ozawa and Kissinger methods.

Table 2
Calculated critical temperature of thermal explosion (T_b) for different samples of HMX obtained from Eq. (4)

		T_b(K)	
Sample no.	T_i(K)	Kissinger	Ozawa
1	551.3	557.45	557.31
2	546.6	554.32	554.11
4	544.5	553.42	553.13
5	539.8	549.85	549.48
6	538.1	548.99	548.56

The critical temperature of thermal explosion (T_b) for each sample of HMX obtained from Eq. (4) are taken from Yang et al. [43] and Zhang et al. [44].

$$T_b = \frac{E_o - \sqrt{E_o^2 - 4E_oRT_{p0}}}{2R} \tag{4}$$

where R is the gas constant ($8.314\,\mathrm{Jmol^{-1}\,K^{-1}}$). E_0 is the value of E obtained by the Ozawa and Kissinger methods. Table 2 shows thermal explosion temperatures for different samples obtained from activation energies calculated by different methods.

Thermodynamic Parameters

The entropy of activation ($\Delta S^{\#}$), enthalpy of activation ($\Delta H^{\#}$), and free energy of activation ($\Delta G^{\#}$) corresponding to $T = T_{\mathrm{p0}}, E = E_a$ and $A = A_{\mathrm{k}}$ obtained by Eqs. (5), (6), and (7) [45–47] for each sample are shown in Table 3.

$$A = \frac{k_B T}{h} e^{\Delta S^{\#}/R} \tag{5}$$

Table 3

Thermodynamic parameters for different samples of HMX: entropy of activation ($\Delta S^{\#}$), enthalpy of activation ($\Delta H^{\#}$), and free energy of activation ($\Delta G^{\#}$) corresponding to $T = T_{p0}, E = E_a$, and $A = A_k$ obtained by Eqs. (5), (6), and (7)

Sample		ΔS (J/mol)		ΔH (kJ/mol)		ΔG (kJ/mol)	
no.	T_i(K)	Kissinger	Ozawa	Kissinger	Ozawa	Kissinger	Ozawa
1	551.3	470.16	478.01	470.15	429.29	210.95	160.80
2	550.0	385.95	402.60	373.05	382.33	160.77	160.9
3	546.6	309.42	326.06	330.67	339.31	161.54	161.72
4	544.5	227.52	244.18	285.44	294.68	161.60	161.72
5	539.8	163.46	180.12	250.17	259.33	161.90	162.10
6	538.1	126.73	147.02	229.86	239.05	161.66	159.84

$$A\exp\left(-\frac{E_a}{RT}\right) = \frac{k_B T}{h}\exp\left(\frac{\Delta S^{\#}}{R}\right)\exp\left(-\frac{\Delta H^{\#}}{RT}\right) \tag{6}$$

$$\Delta G^{\#} = \Delta H^{\#} - T\Delta S^{\#} \tag{7}$$

where k_B is the Boltzmann constant and h is Planck's constant.

Conclusion

The effect of DSC heating rate on the thermal decomposition of HMX at different particle sizes was studied. It was observed that the heating rate is an important factor in the thermal decomposition of HMX. The results show that as the heating rate increases, the decomposition peak shifts to a higher temperature. However, at a constant heating rate, this temperature was decreased as the particle size was reduced. The activation energy and the pre-exponential factor were obtained by the Kissinger and Ozawa methods for all samples. The present study shows that the values of activation energy and pre-exponential factor determined by the Kissinger and Ozawa methods decrease by reducing the particle size of HMX samples. By comparing the activation energy obtained by different methods, it was found that calculated values for various samples by Kissinger's method are lower than those calculated by Ozawa's method.

The critical temperature of thermal explosion of the compound at various particle sizes was calculated. On the other hand, the values of $\Delta S^{\#}$, $\Delta H^{\#}$, and $\Delta G^{\#}$of the reaction at T_{p0} were computed for all samples.

References

[1] Fedoroff, B. T. and O. E. Sheffield. 1966. *Encyclopedia of Explosives and Related Items*. Picatinny Arsenal, NJ: Defense Technical Information Center.

[2] Pinheiro, G. F. M., V. L. Lourenco, and K. Iha. 2002. Influence of the heating rate in the thermal decomposition of HMX. *Journal of Thermal Analysis*, 67: 445–452.

[3] Schroeder, M. 1981. Thermal Decomposition of HMX, Vol. III. Proceedings of the 18th JANNAF Combustion Meeting, Pasadena, California, October 19–23.

[4] Ermolin, N. E. and V. E. Zarko. 1975. Mechanism and Kinetic of the thermal decomposition of cyclic ultramines. *Combustion, Explosion and Shock Waves*, 33: 251.

[5] Rogers, N. R. 1975. Thermochemistry of explosives. *Thermochimica Acta*, 11: 131.

[6] Hussain G. and G. J. Ress. 1995. Thermal decomposition of HMX and mixtures. *Propellants, Explosives, Pyrotechnics*, 20: 74.

[7] Suresh, M., K. Krishnan, and K. N. Ninan. 1998. A DSC study on the effect of RDX and HMX on the thermal decomposition of phase stabilized ammonium nitrate. *Propellants, Explosives, Pyrotechnics*, 23: 150.

[8] Yin, C. M., Z. R. Liu, Y. H. Kong, Y. Luo, S. W. Li, and F. Q. Zhao. 1997. Thermal characteristics of energetic polymers. *Propellants, Explosives, Pyrotechnics*, 29: 356.

[9] Kimura, J. and N. Kubota. 1980. Thermal decomposition process of HMX. *Propellants, Explosives, Pyrotechnics*, 5: 1.

[10] Kissinger, H. E. 1957. Reaction kinetics in differential thermal analysis. *Analytical Chemistry*, 29: 1702.

[11] Ozawa, T. 1970. A modified method for kinetic analysis of thermoanalytical data. *Journal of Thermal Analysis*, 2: 301.

[12] Military Standard, USA, No. 650-T514.1.

[13] Cady, H. H. 1961. *Studies on the Polymorphs of HMX, LAMS-2652*. Los Alamos, New Mexico: Los Alamos Scientific Laboratory.

[14] Cobbledick, R. E. and R. W. H. Small. 1974. The crystal structure of the δ-form of 1, 3, 5, 7-tetranitro-1, 3, 5, 7-tetraazacyclooctane. (δ-HMX). *Acta Crystallographica B*, 30: 1918.

[15] McCrone, W. C. 1950. Crystallographic data. 36. Cyclotetramethylene tetranitramine (HMX). *Analytical Chemistry*, 22: 1225.

[16] Herrmann, M., W. Engel, and N. Eisenreich. 1990. Phase transitions of HMX and their significance for the sensitivity of explosives. Proceedings of the Technical Meeting of Specialists MWDDEA AF-71-F/G-7304—Physics of Explosives, Vienna, Austria, November 13–15.

[17] Karpowicz, R. J. and T. B. Brill. 1982. The based transformation of HMX: Its thermal analysis and relationship to propellants. *AIAA Journal*, 20: 1586.

[18] Teetsov, A. S. and W. C. McCrone. 1965. Microscopial study of polymorph stability diagrams. *Microscope and Crystal Front*, 15: 13.

[19] Herrmann, M., W. Engel, and N. Eisenreich. 1993. Thermal analysis of the phases of HMX using X-ray. *Zeitschrift fürKristallographie*, 204: 121.

[20] Brill, T. B. and R. J. Karpowicz. 1982. Solid phase transition kinetics. The role of intermoleculor forces in the condensed-phase decomposition of octahydro-1,3,5,7-tetranitro-1,3,5,7-tetrazocine. *Journal of Physical Chemistry*, 86: 4260.

[21] Brill, T. B. and C. O. Reese. 1980. Thermal-decomposition of energetic materials. 3. A high-rate, INSITU, FTIR study of the thermolysis of RDX and HMX with pressure and heating rate as variables. *Journal of Physical Chemistry*, 84: 3520.

[22] Mehrotra, P. N., G. V. Chandrashekar, C. N. R. Rao, and E. C. Subbarao. 1966. Hydrodynamic and hydromagenetic stability of viscous-viscoelastic superposed fluids in presence of suspended particles. *Transactions of the Faraday Society*, 62: 3586.

[23] Hall, P. G. 1971. Kirkwood-Buff theory of solutions–alternative derivation of part of A and some applications. *Faraday Transactions*, (Pt 267), 28: 556.

[24] Herrmann, M., W. Engel, and N. Eisenreich. 1992. Thermal expansion, transitions, sensitivities, and burning rates of HMX. *Propellants, Explosives, Pyrotechnics*, 17: 190.

[25] Behrens, R. 1990. Identification of octahydro-1,3,5,7-tetranitro-1,3,5,7-tetrazocine (HMX) pyrolysis products by simultaneous thermogravimetric modulated beam mass spectrometry and time-of-flight velocity-spectra measurements. *International Journal of Chemical Kinetics*, 22: 147–149.

[26] Behrens, R. 1990. Determination of the rates of formation of gaseous products from the pyrolysis of octahydro-1,3,5,7-tetranitro-1,3,5,7-tetrazocine (HMX) by simultaneous thermogravimetric modulated beam mass spectrometry. *International Journal of Chemical Kinetics*, 22: 170–172.

[27] Hosseini, S. G., S. M. Pourmortazavi, and S. S. Hajimirsadeghi. 2005. Thermal decomposition of pyrotechnic mixtures containing sucrose with either potassium chlorate or potassium perchlorate. *Combustion and Flame*, 141: 322–326.

[28] McLain, J. H. and D. V. Lewis. 1965. Effect of Phase Change in Solid-Solid Reactions, Report WCDC 6465, Grant AD-AMC-18–035–77(A), Chemical Research and Development Laboratories, Edgewood Arsenal, MD, May.

[29] McLain, J. H. 1980. *Pyrotechnics from the Viewpoint of Solid State Chemistry*. The Franklin Institute Press.

[30] Fathollahi, M., S. M. Pourmotazavi, and S. G. Hosseini. 2004. The effect of the particle size of potassium chlorate in pyrotechnic compositions. *Combustion and Flame*, 138: 304–306.

[31] Lee, J. S. and C. K. Hsu. 2001. The thermal behaviors and safety chracteristics of composition B explosive. *Thermochimica Acta*, 367–368: 371–374.

[32] Lee, J. S., C. K. Hsu, and C. L. Chang. 2002. A study on the thermal decomposition behaviors of PETN, RDX, HNS, and HMX. *Thermochimica Acta*, 392–393: 173–176.

[33] Pratap, A., K. G. Raval, A. Gupta, and S. K. Kulkarni. 2000. Nucleation and growth of a multicomponent metallic glass. *Bulletin of Materials Science*, 23(3): 185–188.

[34] Zhang, H. and B. Mitchell. 2000. The role of aggregation in crystal growth and transformations in nanophase FeOOH biomineralization products. *Journal of Materials Research*, 15: 1000–1007.

[35] Sha, W. 2001. Determination of activation energy of phase transformation and recrystallization using a modified Kissinger method. *Metallurgical and Materials Transactions A*, 32A: 2903.

[36] Tonbul, Y. and K. Yurdakoc. 2001. Thermogravimetric investigation of the dehydration kinetics of KSF, K10, and Turkish bentonite. *Turkish Journal of Chemistry*, 25: 333–339.

[37] Li, Y., M. Li, and F. Chang. 1999. *Journal of Applied Polymer Science*, 37: 3614–3624.

[38] Pei, C., Z. Qi, L. Yang, H. Zu, G. Li, Z. Mei, D. Zhi, and G. Yin. 2004. Thermal decomposition behavior and non-isothermal decomposition reaction of copper (II) salt of 4-Hydroxy-3,5-dinitro-pyridine oxide and its application in solid rocket propellant. *Chinese Journal of Chemistry*, 22: 1056–1063.

[39] Ali, S., M. H. Bhatti, S. Mahmood, M. Mazhar, M. S. Khalid, and N. Hussan. 1998. Kinetic studies of the thermal decomposition of di- and tri- organotin derivatives of 1-Nitroso-2-Naphthol. *Turkish Journal of Chemistry*, 22: 393–397.

[40] Ozawa, T. 1965. A new method of analysing thermogravimetric data. *Bulletin of the Chemical Society of Japan*, 38: 1881.

[41] Tonglai, Z., H. Rongzu, X. Yi, and L. Fuping. 1994. The estimation of critical temperatures of thermal explosion for energetic materials using non-isothermal DSC. *Thermochimica Acta*, 244: 171–176.

[42] Hai, Z., X. Zhiming, G. Pengjiang, H. Rongzu, G. Shengli, N. Binke, F. Yan, S. Qizhen, and L. Rong. 2002. Estimation of the critical rate of temperature rise for thermal explosion of first-order autocatalytic decomposition reaction systems using non-isothermal DSC. *Journal of Hazardous Materials*, 94: 205–210.

[43] Yang, L., C. Pei, Z. Feng-Qi, H. Rong-Zu, L. Shang-Wen, and G. Yin. 2004. Kinetics and mechanism of the thermal decomposition reaction of 3,3-Bis(azidomethyl)oxetane/tetrahydrofuran copolymer. *Chinese Journal of Chemistry*, 22: 1219–1224.

[44] Zhang, T. L., R. Z. Hu, Y. Xie, and F. P. Li. 1994. The estimation of critical temperatures of thermal explosion for energetic materials using non-isothermal DSC. *Thermochimica Acta*, 244: 171.

[45] Straszko, J., M. Olsok-Humienik, and J. Mozejko. 1997. Kinetics of thermal decomposition of $ZnSO_4 \cdot 7H_2O$. *Thermochimica Acta*, 292: 145.

[46] Olsok-Humienik, M. and J. Mozejko. 2000. Thermodynamic functions of activated complexes created in thermal decomposition processes of sulphates. *Thermochimica Acta*, 344: 73.

[47] Lu, Z. R., Y. C. Ding, Y. Xu, Q. Liu, and J. P. Lang. 2004. *Chinese Journal of Chemistry*, 22: 1091–1094.